Published in final edited form as:
Biomacromolecules. 2011 June 13; 12(6): 2293–2301. doi:10.1021/bm200369e.

Multivalent display of proteins on viral nanoparticles using molecular recognition and chemical ligation strategies

P. Arno Venter[†], **Anouk Dirksen**[‡], **Diane Thomas**[§], **Marianne Manchester**[§], **Philip E. Dawson**[‡], and **Anette Schneemann**[*,†]

[†]Department of Molecular Biology, The Scripps Research Institute, La Jolla, California 92037

[‡]Departments of Cell Biology and Chemistry, The Scripps Research Institute, La Jolla, California 92037

[§]Skaggs School of Pharmacy and Pharmaceutical Sciences, University of California San Diego, California 92093

Abstract

Multivalent display of heterologous proteins on viral nanoparticles forms a basis for numerous applications in nanotechnology, including vaccine development, targeted therapeutic delivery and tissue-specific bio-imaging. In many instances, precise placement of proteins is required for optimal functioning of the supramolecular assemblies, but orientation- and site-specific coupling of proteins to viral scaffolds remains a significant technical challenge. We have developed two strategies that allow for controlled attachment of a variety of proteins on viral particles using covalent and noncovalent principles. In one strategy, an interaction between domain 4 of anthrax protective antigen and its receptor was used to display multiple copies of a target protein on virus-like particles. In the other, expressed protein ligation and aniline-catalyzed oximation was used to covalently display a model protein. The latter strategy, in particular, yielded nanoparticles that induced potent immune responses to the coupled protein, suggesting potential applications in vaccine development.

Keywords

Viral nanoparticle; Flock House virus; virus-like particle; anthrax protective antigen; expressed protein ligation; aniline-catalyzed oxime ligation; vaccine development

Introduction

The extent to which viruses and virus-like particles (VLPs) can be applied in nanotechnology and nanomedicine depends on their ability to serve as effective scaffolds for the multivalent presentation of a wide variety of functional ligands. For certain applications, display of whole proteins or protein domains on the exterior surface of viral particles can be of critical importance. For example, tumor-targeting of viral nanoparticles typically requires display of a protein ligand that recognizes a specific receptor on cells of interest.[1-3] Similarly, applications of viral nanoparticles in bio-imaging may necessitate display of proteins that direct the particle to the relevant site *in vivo*. Another area of research that takes

[*]To whom correspondence should be addressed. Phone: (858) 784-8643. Fax: (858) 784-8643. aschneem@scripps.edu .

Supporting Information Available. Expression analysis of MBP-PA fusion proteins; UV/visible spectra for the products of native chemical ligation and benzaldehyde modification reactions; immunoblot analysis of FHV_{S268K}-MBP conjugates. This material is available free of charge via the Internet at http://pubs.acs.org.

advantage of multivalent display of proteins on viral nanoparticles is vaccine development. Highly effective vaccines induce antibody and T cell responses to multiple epitopes contained within an antigen of interest and this is best achieved if the antigen is presented intact and in its native conformation to the immune system.

The intense interest in viruses and VLPs as platforms for vaccine design is based on the appreciation that viruses display their component proteins in a highly ordered array as a result of the underlying icosahedral or helical symmetry of the particle. Such ordered arrays are known to induce potent antibody responses because they effectively and reliably cross-link B cell receptors.[4] This cross-linking not only leads to a strong IgG response, but often to an extremely rapid T cell-independent IgM response. Harnessing this natural feature of virus particles for development of vaccines against heterologous pathogens has become a key goal. It can be achieved, in principle, by genetic insertion of a protein antigen of interest directly into the structural proteins of the particle but this approach has numerous limitations.[4] Alternatively, purified antigens can be covalently coupled to preformed particles using a variety of bioconjugation methods. A problem with the latter strategy is that it usually results in random orientation of the coupled proteins relative to the particle surface and that the attachment sites on the particle itself may vary from subunit to subunit. Thus, the ordered array necessary for optimal B cell responses is not realized. While coupling multiple copies of proteins in an orientation- and site-specific manner to viral nanoparticles is technically challenging, it has been achieved in a few instances.[1, 2, 5, 6] The strategies used in these cases, however, are either not broadly applicable or require a large excess of substrate over viral nanoparticle because of poor conjugation efficiencies. Valuable protein is thus wasted and large-scale application becomes impractical. The objective of this study was to develop a highly effective conjugation method that reduces the amount of unreacted protein to a minimum, employs low protein concentrations and yields a high percentage of target protein linked to the viral capsid while ensuring site- and orientation-specific attachment.

The viral nanoparticle platform we used is Flock House virus (FHV), a non-enveloped insect RNA virus with T=3 icosahedral capsids made up of 180 identical coat protein subunits.[7, 8] This virus is highly amenable to a variety of biotechnological applications based on its genetic simplicity, exceptional yields and high physicochemical stability, and due to the absence of known safety concerns regarding applications for FHV in animals and humans.[9]

Here we present two approaches that enable the ordered display of proteins by noncovalent or covalent modes of coupling (Figure 1). The noncovalent coupling strategy takes advantage of chimeric FHV particles that permit display of fusion proteins containing domain 4 of anthrax protective antigen (PA) (Figure 1a), while a two-step ligation strategy involving expressed protein ligation (EPL) and aniline-catalized oxime ligation mediates chemoselective ligation of target proteins to viral particles via the covalent method (Figure 1b). A novel and attractive feature common to both strategies is that the protein of interest is expressed in the context of a fusion partner that conveniently aids both in the purification as well as site-specific and orientation-specific attachment of the protein. We demonstrate that these methods enable specific and efficient loading of proteins on the surfaces of viral particles and that the EPL/oxime ligation method yields nanoparticles that induce powerful and rapid immune responses against attached antigen.

Materials and Methods

Construction of plasmids for the expression of maltose binding protein (MBP) and MBP-D4

To generate an *Escherichia coli* expression vector for MBP-D4, a previously described construct comprising FHV protein B2 with an N-terminal MBP tag[10] was cloned into

pET-22b(+) (Novagen). A DNA fragment encompassing the coding sequence of FHV B2 was then excised with BamHI and XbaI and replaced with a corresponding restriction fragment containing PA domain 4 (D4) and a short segment of domain 3 (residues 587-735). This segment was generated by PCR using a previously described expression vector for PA (a generous gift from John Collier, Harvard Medical School, Boston, MA) as a template.[11] The resultant plasmid, called pET-22b(+)MBP-D4, placed an isopropyl-β-D-thiogalactopyranoside (IPTG)-inducible T7 promoter for high-level expression in *E. coli* BL21(DE3) (Novagen) upstream of the coding sequence of C-terminally his-tagged MBP-D4. To generate an expression vector for MBP, a DNA fragment encoding the MalE signal sequence for periplasmic secretion[12] was incorporated into the 5′ end of the reading frame of MBP in pET-22b(+)MBP-D4 via overlap extension PCR[13], followed by removal of the sequence corresponding to PA residues 585-735 by Quikchange mutagenesis (Agilent Technologies).

Purification of MBP, MBP-D4 and PA

E. coli BL21(DE3) cells transformed with DNA vectors for the expression of MBP, MBP-D4 or PA were grown in Luria broth at 37°C to an OD_{600} of 0.6-1.0. For the induction of gene expression, the cultures were grown at 30°C for an additional 4 h in the presence of 1 mM IPTG. Periplasmic extracts for MBP and PA were prepared by osmotic shock according to protocols provided in the pET System Manual (Novagen). Conversely, MBP-D4 expressing cells were disrupted by sonication and centrifuged at 9,000 *g* for 30 min to yield the soluble supernatant fraction. MBP-D4 and MBP were purified from soluble supernatant and periplasmic fractions, respectively, by affinity chromatography using amylose resin (New England Biolabs), while PA was purified from periplasmic extracts by HisTrap column chromatography (GE Healthcare) on an AKTA Purifier (GE Healthcare). Peak fractions containing purified protein were pooled, dialyzed into HBS (10 mM HEPES, pH 7.5, 150 mM NaCl) and stored at −80°C.

Purification of VLPs

Spodoptera frugiperda cells (line IPLB-Sf21)[14] were grown as suspension cultures to a density of 2×10^6 cells/ml at 27°C in Insect-XPRESS medium (Lonza) and then infected at a multiplicity of infection (MOI) of 1 with previously described recombinant baculoviruses AcFHV-VWA_{ANTXR2}-206 or AcFHV-VWA_{ANTXR2}-206 for the synthesis of VNI-206 or VNI-264 VLPs, respectively.[15] At 3 days post-infection, the cells were pelleted by centrifugation at 1,500 *g* for 10 min at 4°C, resuspended in HBS to ¼ of the original volume and disrupted by three passes through an EmulsiFlex C3 homogenizer (Avestin) at a pressure setting ≥ 20,000 psi. Cell debris was pelleted in two steps: first at 13,776 *g* for 10 min at 4°C and then at 100,000 *g* for 10 min at 4°C. VLPs in the clarified supernatant were underlayed with a 3 ml 30% (wt/wt) sucrose cushion in HBS and pelleted by centrifugation in a Beckman 50.2 Ti rotor at 184,048 *g* for 2.5 h at 11°C. The pellets were resuspended in HBS, treated with RNase A (Roche; 6.25 μl of a 10 mg/ml solution per 50 ml original culture volume) for 30 min at 37°C and then centrifuged at 16,100 *g* for 10 min at 4°C. The supernatant was loaded onto 10-40% (wt/wt) sucrose gradients in HBS and centrifuged in a Beckman SW41 rotor at 197,568 *g* for 2.5 h at 11°C. VNI particles were harvested from the gradients by needle puncture.

Synthesis and purification of FHV_{S268K}.particles

Overlap extension PCR was used to introduce an S268K mutation into the coding sequence of wildtype (wt) FHV coat protein on a previously described plasmid called p2BS(+)-wt.[16] The resultant construct served as a template for the synthesis of capped RNA2 transcripts by *in vitro* transcription as described previously.[17] To generate an FHV_{S268K} stock for large-scale FHV_{S268K} preparations, the capped RNA2 transcripts were transfected together with

FHV RNA1 into *Drosophila melanogaster* DL-1 cells using a previously described protocol.[17] The particles were purified from the transfected cells as described previously.[18] Large-scale FHV_{S268K} preparations were carried out by infecting *Drosophila melanogaster* S2 cells at a density of 4×10^7 cells/ml with FHV_{S268K} stock (MOI = 1). Subsequent to the addition of virus, the cells were grown at 27°C in a shake flask at 100 rpm for 1 hour and then diluted 4-fold in growth medium. The cells were incubated for an additional 2 days at 27°C in suspension culture format and then processed for the purification of virus particles as described previously.[18]

Immunoblot analysis of VNI/MBP-D4 complexes

Mixtures of VNI-206 or wt FHV and MBP-D4, MBP or PA were prepared in HBS containing 2 mM $MgCl_2$ at a particle to ligand ratio of 1:90. Following incubation for 1 h at room temperature, the samples were loaded on 5-20% (wt/wt) sucrose gradients in HBS/$MgCl_2$ and centrifuged at 237,020 *g* for 70 min at 11°C in a Beckman SW55 Ti rotor. The pelleted material was resuspended in SDS-PAGE loading buffer, subjected to denaturing SDS-PAGE in NuPage 4-12% gels (Invitrogen) and transferred to nitrocellulose membranes by electroblotting. For two-color detection using an Odyssey infrared imaging system (LI-COR Biosciences), the blots were blocked in blotting buffer (5% nonfat milk in PBS), incubated with mouse anti-His (C- term) antibody (Invitrogen) and rabbit anti-FHV serum in blotting buffer containing 0.1% Tween 20, and washed extensively in PBS/0.1% Tween 20. Goat anti-mouse IR Dye 800CW and goat anti-rabbit IR Dye 680 were used as secondary antibodies following protocols provided by the manufacturer (Odyssey protocol manual, LI-COR Biosciences). The blots were scanned using an Odyssey infrared imaging system (LI-COR Biosciences) and analyzed using its associated Application Software (Version 3).

Electron microscopy

Samples were applied to 300 mesh copper grids with Formvar/Carbon type B support films (Pelco, Ted Pella), washed three times in PBS and stained with 2% uranyl acetate for 1 min. The grids were pretreated in a Solarus model 950 Advanced Plasma Cleaning System (Gatan) prior to sample application. Images were collected at 120 kV using a Tecnai Spirit transmission electron microscope (FEI).

Surface plasmon resonance (SPR) analysis

To determine the binding affinity between MBP-D4 and soluble ANTXR2 (a generous gift from John Young, Salk Institute, La Jolla, CA), SPR analysis was carried out on a Biacore 3000 system (GE Healthcare) using a CM5 sensor chip (GE Healthcare). All experiments were carried out at 25°C in HBS containing 2mM $MgCl_2$ and 0.05% Surfactant P20 (GE Healthcare). Approximately 12,000 response units (RU) of mouse anti-MBP antibody (New England Biolabs) were covalently coupled to the sensor surfaces of flow cells 2-4 using reagents provided in a Biacore Amine Coupling Kit (GE Healthcare). MBP and MBP-D4 were captured in flow cells 3 and 4, respectively, by injecting 300 RU of MBP and 223 RU of MBP-D4 at a flow rate of 100 μl/min, followed by injection of serially diluted ANTXR2 samples using the “Kinject” command into all four flow cells at a flow rate of 40 μl/min. Binding was allowed to occur for 4.5 min and dissociation for 10 min. To regenerate sensor surfaces between measurements, 25 μl 10 mM glycine (pH 2) containing 0.05% P20 surfactant was injected at a flow rate of 50 μl/min using the “Quickinject” command. Regeneration scouting assays showed that the response signal returned to baseline in less than 5 min under these conditions. For kinetic analysis, the binding data was reference-corrected by subtracting sensorgrams resulting from the injection of analyte over MBP-coated surfaces (flow cell 3) from those obtained for MBP-D4-coated surfaces (flow cell 4), normalized to 100 RU and evaluated using BIAevaluation software (GE Healthcare).

Peptide synthesis

Reversed phase high pressure liquid chromatography (RP HPLC) was performed on a Waters Delta Prep 4000 preparative chromatography system (preparative HPLC) and a Phenomenex Jupiter 10μ Proteo 90Å (250 × 21.2 mm) column for separation. Electrospray ionization mass spectrometry (ESI-MS) was performed on a SCIEX API-I single quadruple mass spectrometer.

To synthesize 0.1 mmole bifunctional linker, *t*Boc-C(4-Me-Bzl)GGK(Fmoc)-MBHA resin was obtained *via* manual solid phase peptide synthesis (SPPS) using an *in situ* neutralization/1*H*-benzotriazolium-1-[bis(dimethylamino)methylene]-5-chloro-hexafluorophosphate-(1-),3-oxide (HCTU) activation procedure for *t*Boc chemistry on a *p*-methylbenzhydrylamine (MBHA) resin (0.65 meq/g).[19] The Fmoc protecting group of the C-terminal lysine residue of *t*Boc-C(4-Me-Bzl)GGK(Fmoc) was removed on the resin by treatment with 20% (vol) 4-methylpiperidine in DMF (4 × 3 min) followed by a DMF flow wash. 0.5 mmol (96 mg) *t*Boc-aminooxyacetic acid was added to a solution of 0.5 mmol (63 mg) diisopropylcarbodiimide (DIC) and 0.5 mmol (58 mg) *N*-hydroxysuccinimide in 1 mL of DMF (no preactivation) and the mixture was added to the resin (2 hours). The resin was washed with DMF and the *t*Boc groups were removed with trifluoroacetic acid (TFA) (2 × 1 min). The resin was washed with DMF and DCM and dried under vacuum. The peptide was cleaved from the resin by HF using 4% (vol) of anisole as a scavenger. After lyophilization, the bifunctional linker was purified by RP HPLC (gradient: 0 - 25% 9:1 *v/v* MeCN/H_2O in H_2O, 0.1% (vol) TFA in 80 min; flow: 20 mL/min). ESI-MS calcd. for 15H29N7O6S ($[M+H]^+$): 435.5, found 435.5.

Expressed protein ligation

To purify MBP-intein, BL21(DE3) cells transformed with pMXB10 (New England Biolabs) were grown in Luria broth at 37°C to an OD_{600} of 0.6-1.0, induced for 4 hours at 30°C in the presence of 1 mM IPTG and disrupted by sonication. The cell lysate was centrifuged at 15,000 *g* for 30 min and resultant clarified supernatant loaded on a chitin bead column (New England Biolabs). The column was washed with 20 bed volumes of column buffer (20 mM HEPES, pH 8.5, 500mM NaCl) and on-column cleavage was induced by rapidly flushing 3 bed volumes of column buffer containing 50 mM mercaptoethanesulfonic acid (MESNA) through the column, stopping column flow and incubating the column overnight at 4°C. C-terminally thioester-tagged MBP was eluted from the column using column buffer, dialyzed into 5 mM Bis Tris (pH 6.5), 250 mM NaCl and stored at −80°C.

To generate aminooxy-derivatized MBP (MBP-AO), 10 μM thioester-tagged MBP was reacted overnight at 4°C with 100-fold excess peptide linker in 100 mM Tris buffer (pH 8.5) containing 10 mM MESNA. Unincorporated peptide was removed by buffer exchange into 100 mM sodium phosphate buffer (pH 6.5) and the MBP-AO product concentrated to 100 μM using 10 kDa cut-off centrifugal filter devices (Amicon, Millipore). To estimate the efficiency of MBP-AO formation, 50 μM MBP-AO was reacted with 2-fold excess 4-formylbenzoyl-PEG3-fluorescein (Solulink) in the presence of 100 mM aniline for 48 h at room temperature. Thioester-tagged MBP served as a control for this reaction. The mixtures were loaded on an amylose resin column (New England Biolabs), washed with 30 volumes of 20 mM Tris, pH 7.4, 200 mM NaCl and eluted using the same buffer containing 10 mM maltose. The level of aminooxy-derivatized peptide incorporation was indirectly determined by measuring the absorbance of fluorescein at 494 nm, using a measured ε of 41,664 $M^{-1}cm^{-1}$ at pH 7.4 for 4-formylbenzoyl-PEG3-fluorescein.

Benzaldehyde modification

FHV_{S268K} particles were subjected to buffer exchange into 100 mM sodium phosphate buffer (pH 7.4) and concentrated to 2.5 mg/ml using 100 kDa cut-off centrifugal filter devices (Amicon, Millipore). The particles were incubated with 5 mM sulfo-succinimidyl 4-formylbenzoic acid (sulfo-S-4FB, Solulink) for 2 h at room temperature. The benzaldehyde-modified FHV_{S268K} particles were purified by buffer exchange into 100 mM sodium phosphate buffer (pH 6.5) and concentrated to 2.5 mg/ml, which corresponded to 48μM surface-exposed benzaldehyde groups assuming 100% conjugation efficiency. Benzaldehyde modification was quantified with 2-hydrazinopyridine according to protocols supplied by the manufacturer (Solulink). Addition of this compound to sulfo-S-4FB-modified biomolecules results in the formation of a bis-aryl hydrazone bond which absorbs at 350 nm. The fraction of surface exposed lysines on FHV_{S268K} with attached benzaldehyde groups was calculated by subtracting the number of benzaldehyde groups per wt FHV particle from the number of these groups incorporated per FHV_{S268K} particle.

Oxime ligation

MBP-AO (50 μM) was incubated with 1.25 mg/ml benzaldehyde-derivatized FHV_{S268K} (~25 μM surface-exposed benzaldehydes) in 100 mM sodium phosphate buffer (pH 6.5) containing 100 mM aniline for 48 h at room temperature. The reaction mixtures were then subjected to size exclusion chromatography (SEC) on a Superdex 200 10/300 GL column (GE Healthcare) using HBS as a running buffer. This column efficiently separated unconjugated MBP from FHV_{S268K}-MBP conjugate, which eluted in the void volume. Aliquots of fractions comprising the flow-through peak were electrophoresed through a NuPage 4-12% gel (Invitrogen) and the gel was stained with Simply Blue (Invitrogen). The loading of MBP on the surface of FHV_{S268K} particles was determined by densitometric analysis using FluorChem SP (Alpha Innotech) in which the relative intensities of bands corresponding to coat protein-MBP conjugate and free coat protein were compared for each lane.

Immunogenicity studies

Immunization studies were carried out in 6 week old, male Balb/cByJ mice according to protocols approved by the Scripps Institutional Animal Care and Use Committee. For studies employing VNI/MBP-D4 complexes, mice (6 per group) were injected subcutaneously with 100 μl HBS/2mM $MgCl_2$ containing either 9.4 μg VNI-264/MBP-D4 complex (particle to ligand ratio of 1:120), 8.5 μg VNI-206/MBP-D4 complex (particle to ligand ratio of 1:90), or 3.6 μg MBP-D4 (molar equivalent of MBP-D4 complexed with VNI-264). A control group received buffer only. For immunization studies employing FHV-MBP conjugates, mice (4 per group) were inoculated subcutaneously with 100 μl PBS containing either 10 μg FHV_{S268K}-MBP or 3.3 μg MBP (molar equivalent of MBP linked to FHV_{S268K} assuming 90 copies/particle). A control group was inoculated with PBS only. All animals were immunized twice in an interval of three weeks. Mice were anesthetized with isofluorane before all procedures. Serum was prepared from whole blood collected from the submandibular vein prior to immunization, as well as 3 weeks and 6 weeks post immunization.

ELISA

Immulon microtiter 96-well plates (Thermo Scientific) were coated overnight with 10 μg/ml MBP in 100 mM $NaHCO_3$, pH 8.5 (100 μl/well). ELISAs were performed as described previously,[15] with the exception that horseradish peroxidase-conjugated goat anti-mouse antibodies (Jackson ImmunoResearch) were used for secondary immunodetection. Specific antibody binding was quantified by addition of 100 μl soluble TMB substrate solution

(Calbiochem, Merck) to each well and incubation at 37°C for 10 min. Color development was stopped by addition of 100 μl 1N HCl to each well and the signal was quantified at 450 nm using a Versamax microplate reader (Molecular Devices).

Statistics

Results are expressed as mean ± standard deviation. A Student's paired *t* test was used for statistical analysis.

Results and Discussion

Design and synthesis of MBP-PA fusion proteins

FHV VLPs were previously engineered to multivalently display 180 copies of the anthrax toxin receptor ANTXR2 on their surface.[15] This was accomplished by genetic insertion of the sequence of the von Willebrand factor type A (VWA) domain of ANTXR2 at amino acid position 206 or 264 of FHV coat protein. The resultant VLPs, designated VNI-206 or VNI-264, respectively, function as efficient ligands for anthrax PA, one of the two components of the bipartite anthrax toxins. As a result, they neutralize PA and protect cells from *in vitro* intoxication.[15] In addition, complexes formed between VNI-264 and PA induce a potent neutralizing antibody response against PA that protects rats from lethal anthrax toxin challenge after a single immunization in the absence of adjuvants.[15]

We sought to expand the VNI platform for non-covalent display of protein ligands other than PA by taking advantage of the molecular recognition between ANTXR2 and PA (Figure 1a). Specifically, we explored whether the region of PA involved in binding to ANTXR2 VWA domains on VNI particles could serve as an adapter for the multivalent display of other proteins of interest. PA is structurally organized into four domains, two of which, domains 2 and 4, are involved in attachment to ANTXR2 (Figure 2a).[20] To determine whether truncated versions of PA could serve as an adapter for VNI attachment, fusions between maltose-binding protein (MBP) and various N-terminally deleted mutants of PA were expressed in *E. coli*. MBP served as a convenient model antigen for these studies due to its ease of expression and purification by amylose affinity chromatography. In addition, amylose affinity chromatography provided a useful indicator to gauge whether MPB in the context of a fusion with PA retained its native conformation. Of the MBP-PA fusions that were tested, high yields of pure, soluble protein were only obtained for MBP-D4, a construct retaining PA domain 4 (D4) and a short segment of domain 3 (residues 587-735, approx. 18 kDa) (Figure 2b and supporting information, Figure S1).

Noncovalent coupling of MBP-D4 to the VNI platform

The binding of D4 to ANTXR2 is mediated by a direct interaction between aspartate-683 in PA and a divalent metal ion-dependent adhesion site in ANTXR2 (Figure 2a). This interaction in combination with an additional binding surface provided by PA domain 2 is responsible for the exceptionally high affinity of PA for its receptor (K_d = 170 pM).[21-24] To test if D4 sufficed for binding of proteins to VNIs, mixtures of VNI-206 and MBP-D4 were incubated in the presence of 2 mM Mg^{++}, followed by pelleting through a sucrose gradient to remove unbound ligand and immunoblot analysis of the resultant pellet. PA and MBP were used as positive and negative control ligands, respectively. The mixtures had a particle to ligand ratio of 1:90, matching the previously determined occupancy of PA on VNI-206.[15] As anticipated, in the absence of VNI-206 none of the three ligands were detectable in the pellet after sucrose gradient centrifugation (Figure 2c, lanes 6-8). In contrast, bands with roughly equivalent intensities were detected for both PA and MBP-D4 when VNI-206 was present in the mixture (Figure 2c, lanes 9 and 11). This demonstrated that MBP-D4 efficiently bound to VNI-206 and that the complexes were stable during ultracentrifugation.

Binding of MBP-D4 to VNI-206 was also confirmed by electron microscopy (EM), which revealed distinct protrusions emanating from the surfaces of VNI-206 compared to VNI-206 in the absence of MBP-D4 (Figure 2e). The inability of MBP to co-pellet with VNIs (Figure 2c, lane 10) and MBP-D4 to co-pellet with wt FHV (Figure 2d) made it evident that the binding of MBP-D4 to VNI-206 was dependent on interaction between D4 and ANTXR2. Analogous results were obtained for VNI-264, using a particle to ligand ratio of 1:120, the previously determined occupancy of PA on this type of particle (data not shown).

Binding kinetics of MBP-D4 to ANTXR2

Surface plasmon resonance (SPR) was employed to determine the binding affinity between MBP-D4 and ANTXR2. To this end, MBP-D4 was immobilized on a sensor chip through a covalently linked anti-MBP antibody, and soluble ANTXR2 was passed over the surface.[23] An MBP-coated sensor served as a reference cell for background subtraction. Global fit analysis of sensorgrams resulting from the injection of different concentrations of ANTXR2 showed that the binding data conformed to 1:1 Langmuir binding (Figure 3) and a K_d of 81 nM was determined from the calculated association and dissociation rate constants. This value, while lower than the affinity of PA for ANTXR2, was similar to those of other receptor-ligand combinations that have previously been proven to be effective for applications in vaccine development.[25-28]

Covalent coupling of MBP to FHV via EPL/oxime ligation

A second approach for site-specific and orientation-specific antigen display was developed using covalent attachment of MBP to FHV particles. This chemical ligation approach involved addition of an aminooxy-derivatized peptide to the C-terminus of MBP via EPL[29] and subsequent site-specific coupling of the functionalized product to benzaldehyde-derivatized FHV particles using aniline-catalyzed oxime ligation[30-32] (Figure 1b). Specifically, a fusion between MBP and an intein protein-splicing element was expressed in *E. coli* and bound to a chitin affinity column via a chitin-binding domain contained within the sequence of the intein. Induction of on-column cleavage using MESNA resulted in generation of MBP with a C-terminal thioester (Figure 1b, product 1).[29] The modified MBP (10μM) was then coupled to the N-terminal cysteine of an aminooxy-derivatized bifunctional linker (1 mM; compound 2 in Figure 1b) using native chemical ligation.[33-34] This amide forming ligation reaction allowed for incorporation of aminooxy moieties into MBP with 43±10% efficiency as indicated by subsequent quantitative oxime ligation using an excess of 4-formylbenzoyl-PEG3-fluorescein (see Supporting Information, Figure S2).

Coupling of the aminooxy-derivatized MBP (MBP-AO; product 3 in Figure 1b) to FHV required functionalization of the exterior surface of the virus particle with reactive groups. We used sulfo-succinimidyl 4-formylbenzoic acid (sulfo-S-4FB) and an FHV mutant particle bearing an S268K point mutation to provide solvent-accessible lysine residues for conjugation of benzaldehyde groups to the viral protein subunits (Figure 1b). The reaction saturated the 180 surface-exposed lysine residues with the reactive groups as determined spectroscopically by incubation of the sulfo-S-4FB-derivatized particles with 2-hydrazinopyridine and measurement of hydrazone bond formation at a wavelength of 350 nm (see Supporting Information, Figure S3).

To generate covalent FHV-MBP conjugates, MBP-AO (~50μM) and benzaldehyde-derivatized FHV_{S268K} (Figure 1b; product 4) were ligated in the presence of 100mM aniline at a 2:1 molar ratio of MBP-AO to surface exposed benzaldehyde groups. The conjugates were purified by SEC and characterized by SDS-PAGE, immunoblot analysis and EM. Viral nanoparticle yield was 52±7% subsequent to oxime ligation and SEC. SDS-PAGE analysis showed substantial quantities of the desired MBP-FHV ligation product (Figure 1b, product

5), evident from an intense band migrating at the combined molecular weight (~80 kDa) of MBP and FHV coat protein (Figure 4a, lane 4). Immunoblot analysis confirmed the presence of both FHV coat protein and MBP within this ligation product (Supporting information, Figure S4). In contrast, negligible amounts of coat protein-MBP conjugate were detectable in a control experiment, in which wt FHV was used instead of FHV_{S268K} for the benzaldehyde/MBP-AO coupling reaction (Figure 4a, lane 2). This result demonstrated that surface-exposed benzaldehyde groups were required for efficient attachment of MBP-AO to the particles and that wt FHV, which does not contain surface-exposed lysines according to its crystal structure, contains small amounts of unidentified side chain groups that can react with sulfo-S-4FB. In addition to the major MBP-FHV ligation product, two faster migrating proteins were also detected in the FHV_{S268K}-MBP conjugates (Figure 4a, lane 4). These protein species represented coat protein subunits which had not reacted with MBP-AO as confirmed by immunoblot analysis (Supporting information, Figure S4). Note that FHV coat protein is typically detected as a faster and a slower migrating form during SDS-PAGE, depending on the maturation state of the particle.[35] Trace amounts of monomeric MBP were also detectable in the FHV_{S268K}-MBP conjugates as well as a small quantity of non-specific multimers with molecular weights of ~120 kDa and higher consisting of coat protein and MBP subunits (Figure 4a, lane 4 and Figure 4S). The reasons underlying the presence of these unanticipated protein species in the purified viral conjugates remain to be determined.

Correcting for the molecular masses of unmodified coat protein and MBP-coat protein conjugates, a loading of 100±6 MBP molecules per particle was determined by densitometry analyses of Coomassie-stained SDS-PAGE gels for two independent FHV_{S268K}-MBP preparations. Examination of the conjugates by EM confirmed that they represented intact particles (Figure 4b). Compared to the smooth exterior of FHV_{S268K} virions, the surface of FHV_{S268K} particles conjugated to MBP was rough and distinct protrusions were visible. Taken together, these data established that oxime ligation of aminooxy-modified proteins is an efficient strategy to selectively attach proteins to viral particles for multivalent display.

Immunization studies with MBP-coated nanoparticles

We next tested whether multivalent display of MBP on viral nanoparticles, either through covalent attachment or non-covalent molecular recognition, would induce a more robust anti-MBP immune response than monomeric MBP. In the first study, mice were immunized with either 9.4 μg VNI-264/MBP-D4 complex (particle to ligand ratio of 1:120), 8.5 μg VNI-206/MBP-D4 complex (particle to ligand ratio of 1:90), or 3.6 μg MBP-D4 (molar equivalent of MBP-D4 complexed with VNI-264). The immunization schedule involved two subcutaneous injections at weeks 0 and 3 in the absence of adjuvant. Blood was collected prior to each injection as well as three weeks after the second injection. ELISA of pre- and post-inoculation sera showed that some animals immunized with VNI-206/MBP-D4 or VNI-264/MBP-D4 contained high levels of anti-MBP antibody after boosting (Figure 5a). However, on average, neither of these complexes induced significantly increased anti-MBP responses when compared to MBP-D4 alone, either at week 3 or after boosting (Figure 5a). A possible explanation for the inability of VNI/MBP-D4 complexes to elicit reliably strong antibody responses might have been the decreased affinity between VNI and MBP-D4 and the dependence of the interaction on divalent cations. If the concentration of Mg^{++} *in vivo* is limiting, local conditions encountered by the complexes may favor their dissociation with a resultant loss of multivalency of the antigen of interest. Avenues are potentially available to enhance the stability of VNI/D4 complexes for *in vivo* applications. For example, mutations in the D4 contact site on ANTXR2 have been identified that should increase the binding affinity of VWA domains on VNIs for D4.[36]

In contrast, vaccination with covalent FHV_{S268K}-MBP conjugates resulted in significantly higher anti-MBP responses when compared to animals receiving monomeric MBP even

after the first injection (week 3, $p = 0.005$) (Figure 5b). The booster injection further potentiated the anti-MBP response with average ELISA readings at least 5.9 fold higher than the mean for MBP-immunized mice (Figure 5b). The strong and rapid anti-MBP responses observed for FHV_{S268K}-MBP demonstrated that the EPL/oxime ligation strategy described here represents an effective method to link whole protein antigens to viral nanoparticles in a manner that is stable under *in vivo* conditions and that the resulting complexes are far superior at inducing an immune response to the protein of interest compared to its monomeric form. Most importantly, the strong and rapid anti-MBP response observed for FHV_{S268K}-MBP is reminiscent of that previously observed for a highly effective FHV-based vaccine that offered protective immunity from anthrax lethal toxin challenge.[15] The EPL/oxime ligation strategy therefore holds significant promise for the development of novel vaccines against toxins and pathogens for which rapid and protective immune responses are urgently needed.

Conclusion

We have developed two methods aimed at increasing the efficiency with which protein ligands can be coupled to the exterior surface of viral nanoparticles in an orientation- and site-specific manner. In the molecular recognition method a strong metal ion-dependent interaction with a K_d of ~80 nM was used to couple 90 or 120 target molecules, representing the protein of interest fused to domain 4 of anthrax PA, to two different types of FHV VLPs displaying the VWA domain of ANTXR2. This non-covalent strategy is applicable to proteins that can be expressed as a fusion with D4. Given the small size of D4, we anticipate this to be possible for a wide variety of polypeptides. In fact, we have already generated derivatives of botulinum neurotoxin A coupled to D4 and shown them to bind to VNIs with the same efficiency as MBP-D4. The non-covalent strategy is exceptionally economical as each substrate monomer will bind to the nanoparticle platform until saturation is reached. The amount of protein required to reach saturation can be precisely determined thus eliminating the losses typically encountered in reactions requiring covalent bond formation.

Although the non-covalent strategy did not yield enhanced IgG responses to the target antigen, it is possible that this could be achieved by increasing the affinity between PA domain 4 and ANTXR2. The complexes should also be compatible with a variety of *in vitro* applications. For example, the ordered array on the VNI platform can be expected to allow rapid, subnanometer structure determination of the bound proteins using cryo-electron microscopy and image reconstruction, given the size and icosahedral symmetry of the nanoparticle platform. Investigations to this end are currently underway in our laboratory.

In contrast, the EPL/oxime ligation strategy allowed covalent coupling of approximately 100 target molecules to the surface of FHV. Because EPL and oxime ligation have already been employed to couple proteins and peptides to numerous monomeric protein targets,[33, 37-39] we believe that this approach will also have broad applicability for coupling proteins to viral nanoparticles. It merely requires expression of a protein of interest with an intein tag, a suitable peptide linker and the presence of a lysine residue on the surface of the nanoparticle of choice. The latter can be easily engineered into the capsid if not present in the native protein as we have done for FHV.

The EPL/oxime ligation strategy offers additional advantages over other reported methods for site- and orientation-specific bioconjugation. Oxime ligation reactions are chemoselective and compatible with a wide range of biomolecules, based on the mild nature of aniline as a biocatalyst. Most importantly, this strategy requires only low micromolar reactant concentrations. In our study, a twofold molar excess of protein substrate over functional groups on the nanoparticle yielded 55% coupling efficiency using 25-50 μM

protein concentrations. These conditions can be further optimized. Notably, the EPL/oxime ligation strategy yields nanoparticles that induce potent immune responses against the coupled protein suggesting potential applications in vaccine development.

Supplementary Material

Refer to Web version on PubMed Central for supplementary material.

Acknowledgments

This study was supported by NIH grant AI080965 to A.S. and M.M. and International Aids Vaccine Initiative grant SFP-1851R to P.E.D. We thank Nicholas Brunn for technical assistance with the preparation of VNI particles.

REFERENCES

1. Banerjee D, Liu AP, Voss NR, Schmid SL, Finn MG. Chembiochem. 2010; 11(9):1273–1279. [PubMed: 20455239]
2. Chatterji A, Ochoa W, Shamieh L, Salakian SP, Wong SM, Clinton G, Ghosh P, Lin T, Johnson JE. Bioconjugate Chem. 2004; 15(4):807–813.
3. Huang RK, Steinmetz NF, Fu CY, Manchester M, Johnson JE. Nanomedicine (London, U.K.). 2011; 6(1):55–68.
4. Jennings GT, Bachmann MF. Biol. Chem. 2008; 389(5):521–536. [PubMed: 18953718]
5. Jegerlehner A, Tissot A, Lechner F, Sebbel P, Erdmann I, Kundig T, Bachi T, Storni T, Jennings G, Pumpens P, Renner WA, Bachmann MF. Vaccine. 2002; 20(25-26):3104–3112. [PubMed: 12163261]
6. Strable E, Finn MG. Curr. Top. Microbiol. Immunol. 2009; 327:1–21. [PubMed: 19198568]
7. Fisher AJ, Johnson JE. Nature. 1993; 361(6408):176–179. [PubMed: 8421524]
8. Venter, PA.; Jovel, J.; Schneemann, A. Insect nodaviruses. In: Asgari, S.; Johnson, KN., editors. Insect Virology. Caister Academic Press; Norfolk, U.K.: 2010.
9. Venter PA, Schneemann A. Cell. Mol. Life Sci. 2008; 65(17):2675–2687. [PubMed: 18516498]
10. Chao JA, Lee JH, Chapados BR, Debler EW, Schneemann A, Williamson JR. Nat. Struct. Mol. Biol. 2005; 12(11):952–957. [PubMed: 16228003]
11. Benson EL, Huynh PD, Finkelstein A, Collier RJ. Biochemistry. 1998; 37(11):3941–3948. [PubMed: 9521715]
12. Choi JH, Lee SY. Appl. Microbiol. Biotechnol. 2004; 64(5):625–635. [PubMed: 14966662]
13. Horton RM, Ho SN, Pullen JK, Hunt HD, Cai Z, Pease LR. Methods Enzymol. 1993; 217:270–279. [PubMed: 8474334]
14. Vaughn JL, Goodwin RH, Tompkins GJ, McCawley P. In Vitro. 1977; 13(4):213–217. [PubMed: 68913]
15. Manayani DJ, Thomas D, Dryden KA, Reddy V, Siladi ME, Marlett JM, Rainey GJ, Pique ME, Scobie HM, Yeager M, Young JA, Manchester M, Schneemann A. PLoS Pathog. 2007; 3(10):1422–1431. [PubMed: 17922572]
16. Schneemann A, Zhong W, Gallagher TM, Rueckert RR. J. Virol. 1992; 66(11):6728–6734. [PubMed: 1404613]
17. Schneemann A, Marshall D. J. Virol. 1998; 72(11):8738–8746. [PubMed: 9765417]
18. Marshall D, Schneemann A. Virology. 2001; 285(1):165–175. [PubMed: 11414816]
19. Schnolzer M, Alewood P, Jones A, Alewood D, Kent SB. Int. J. Pept. Protein Res. 1992; 40(3-4):180–193. [PubMed: 1478777]
20. Petosa C, Collier RJ, Klimpel KR, Leppla SH, Liddington RC. Nature. 1997; 385(6619):833–838. [PubMed: 9039918]
21. Scobie HM, Rainey GJ, Bradley KA, Young JA. Proc. Natl. Acad. Sci. U. S. A. 2003; 100(9):5170–5174. [PubMed: 12700348]

22. Scobie HM, Wigelsworth DJ, Marlett JM, Thomas D, Rainey GJ, Lacy DB, Manchester M, Collier RJ, Young JA. PLoS Pathog. 2006; 2(10):e111. [PubMed: 17054395]
23. Wigelsworth DJ, Krantz BA, Christensen KA, Lacy DB, Juris SJ, Collier RJ. J. Biol. Chem. 2004; 279(22):23349–23356. [PubMed: 15044490]
24. Young JA, Collier RJ. Annu. Rev. Biochem. 2007; 76:243–265. [PubMed: 17335404]
25. Li Q, Shivachandra SB, Leppla SH, Rao VB. J. Mol. Biol. 2006; 363(2):577–588. [PubMed: 16982068]
26. Li Q, Shivachandra SB, Zhang Z, Rao VB. J. Mol. Biol. 2007; 370(5):1006–1019. [PubMed: 17544446]
27. Shivachandra SB, Li Q, Peachman KK, Matyas GR, Leppla SH, Alving CR, Rao M, Rao VB. Vaccine. 2007; 25(7):1225–1235. [PubMed: 17069938]
28. Shivachandra SB, Rao M, Janosi L, Sathaliyawala T, Matyas GR, Alving CR, Leppla SH, Rao VB. Virology. 2006; 345(1):190–198. [PubMed: 16316672]
29. Muralidharan V, Muir TW. Nat. Methods. 2006; 3(6):429–438. [PubMed: 16721376]
30. Dirksen A, Dawson PE. Curr. Opin. Chem. Biol. 2008; 12(6):760–766. [PubMed: 19058994]
31. Dirksen A, Dawson PE. Bioconjugate Chem. 2008; 19(12):2543–2548.
32. Dirksen A, Hackeng TM, Dawson PE. Angew. Chem. Int. Ed. Engl. 2006; 45(45):7581–7584. [PubMed: 17051631]
33. Flavell RR, Kothari P, Bar-Dagan M, Synan M, Vallabhajosula S, Friedman JM, Muir TW, Ceccarini G. J. Am. Chem. Soc. 2008; 130(28):9106–9112. [PubMed: 18570424]
34. Dawson PE, Muir TW, Clark-Lewis I, Kent SB. Science. 1994; 266(5186):776–779. [PubMed: 7973629]
35. Gallagher TM, Rueckert RR. J. Virol. 1988; 62(9):3399–3406. [PubMed: 3404580]
36. Scobie, HM. PhD Thesis in Cellular and Molecular Biology. University of Wisconsin-Madison; 2006. Anthrax toxin receptors and soluble receptor-based antitoxins.
37. Berrade L, Camarero JA. Cell. Mol. Life Sci. 2009; 66(24):3909–3922. [PubMed: 19685006]
38. Singla N, Erdjument-Bromage H, Himanen JP, Muir TW, Nikolov DB. Chem. Biol. 2011; 18(3): 361–371. [PubMed: 21439481]
39. Zeng Y, Ramya TN, Dirksen A, Dawson PE, Paulson JC. Nat. Methods. 2009; 6(3):207–209. [PubMed: 19234450]

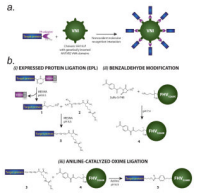

FIGURE 1.

Schematic diagram of strategies allowing orientation- and site-specific presentation of whole proteins on FHV-based nanoparticles. (a) Noncovalent attachment: the target protein is expressed as a fusion with a fragment of PA that is required for binding to ANTXR2. A C-terminal polyhistidine (his) tag allows purification via Ni-affinity chromatography. Multivalent display is achieved by binding of the fusion protein to VNIs, which display 180 copies of ANTXR2 on their surface. (b) Covalent attachment: the target protein is expressed with an intein tag and immobilized on a chitin affinity column via a chitin-binding domain (CBD). Subsequent to intein-mediated thiolysis, the target protein is released from the intein with a C-terminal thioester group (**1**), which is then conjugated via native chemical ligation to a heterobifunctional peptide linker (**2**), to generate an aminooxy-derivatized product (**3**). Coupling of this product to FHV requires benzaldehyde groups on derivatized FHV mutant S286K containing 180 surface exposed lysines (**4**). An aniline-catalyzed oxime ligation reaction between products (**3**) and (**4**) yields FHV-based nanoparticles displaying multiple copies of the target protein (**5**).

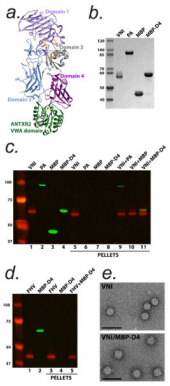

FIGURE 2.

Binding of MBP-D4 to VNI particles. (a) Ribbon diagram of PA bound to ANTXR2. The divalent metal ion in ANTXR2 (green) required for binding of PA domain 4 (purple) is depicted as a golden sphere. The side chain of Asp683 in PA domain 4, which contacts the metal ion directly, is also shown. Arrows (orange) point to amino acid positions of PA where the protein was fused to the C terminus of MBP: glycine-241 (top left), proline-254 (top right) and methionine-585 (bottom). Fusions at positions 241 and 254 retain domains 2, 3 and 4, while fusion at methionine-585 preserves domain 4 and a short segment of domain 3. For additional data about the expression and purification of these MBP-PA fusion proteins refer to Figure S1 (Supporting Information). (b) Electrophoretic analysis of purified VNI-206, PA, MBP and MBP-D4 on an SDS-PAGE gel stained with Simply Blue (Invitrogen). The two protein species detected for VNI-206 represent the unprocessed precursor form of the chimeric coat protein (minor band) and its cleaved product (major band). (c) Centrifugation-based assay to determine ability of MBP-D4 to bind to VNI-206. Mixtures comprising VNI-206 and either MBP-D4, MBP or PA were incubated for 1 hour at room temperature in the presence of 2 mM Mg^{++}, then subjected to ultracentrifugation through a sucrose gradient to remove unbound ligand. Western blot analysis of the resultant pellets was performed with an anti-his tag antibody to detect PA, MBP and MBP-D4 (green) and FHV antiserum to detect coat protein subunits of VNI-206 (red). Lanes 1-4 are controls showing the fluorescent signal for the input samples relative to those recovered in the pellets shown in lanes 5-11. Lanes 5-8: samples indicated at the top were separately centrifuged through the gradient. Only VNI-206 is detectable in the pellet (lane 5). Lanes 9-11: samples indicated at the top were mixed and centrifuged through the gradient. In addition to VNI-206, PA and MBP-D4 are detectable in the pellet, but not MBP. (d) Centrifugation-based assay showing that MBP-D4 does not bind to wt FHV particles. Lanes 1 and 2: controls analogous to those shown in lanes 1-4 of part (c). Lanes 3-5: samples indicated at the top were centrifuged through a sucrose gradient. Only FHV protein is detected in the pellets. (e) Electron micrographs of VNI-206 particles and VNI-206/MBP-D4 complexes (scale bar, 100 nm).

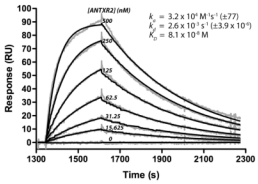

FIGURE 3.

SPR analysis to determine the binding affinity of MBP-D4 for ANTXR2. The gray traces represent sensorgrams for the injection of six different concentrations of a soluble ANTXR2 over the sensor surface, and the black lines show the results of global fit analysis using a 1:1 Langmuir binding model. Observed association rate (k_a), dissociation rate (k_d) and equilibrium dissociation (K_d) constants are indicated. The figure represents data from one of two independent binding experiments with similar results.

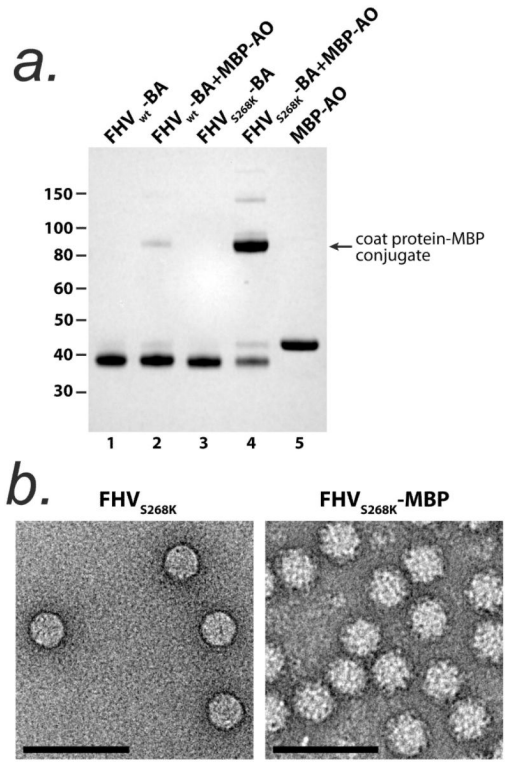

FIGURE 4.

Characterization of FHV_{S268K}-MBP conjugates. (a) SDS-PAGE analysis of size exclusion chromatography purified conjugates prepared by aniline-catalyzed oximation reactions between benzaldehyde-modified wt FHV (FHV_{wt}-BA) or FHV_{S268K} particles (FHV_{S268K}-BA) and aminooxy-derivatized MBP (MBP-AO). (b) Electron micrographs of FHV_{S268K} particles and FHV_{S268K} -MBP conjugates (scale bar, 100 nm).

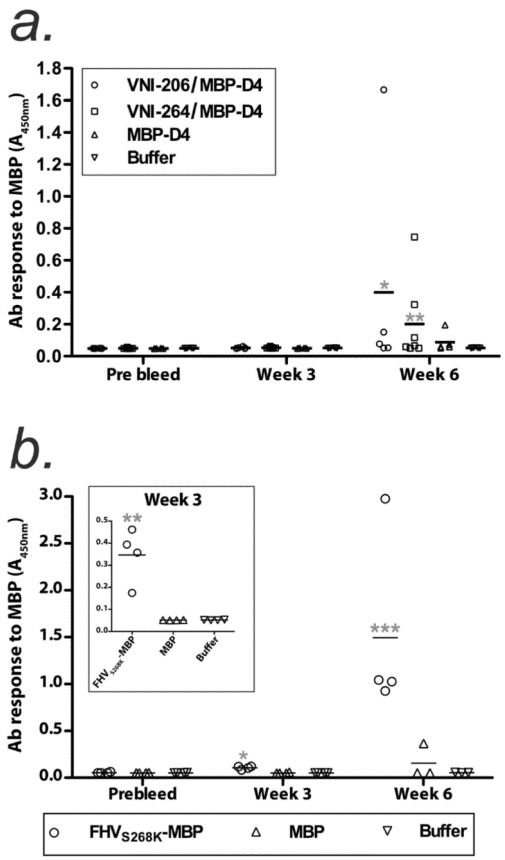

FIGURE 5.

IgG-specific antibody response to MBP in mice vaccinated with FHV-based nanoparticles. (a) Mice (six per group) were immunized subcutaneously with VNI-206/MBP-D4 complex, VNI-264/MBP-D4 complex, MBP-D4 alone or buffer (HBS containing 2mM $MgCl_2$), and boosted 3 weeks later. Presence of IgG-specific anti-MBP antibodies in sera prior to immunization, as well as 3 and 6 weeks post-immunization was determined by ELISA using 1:100 serum dilution. Data points represent anti-MBP antibody levels of individual animals, while horizontal bar represents average value for each group. At week 6, * and ** indicate *p* values of 0.381 and 0.299 compared to MBP-D4 alone, respectively. (b) Mice (four per group) were immunized and boosted 3 weeks later with FHV_{S268K} - MBP conjugate, MBP alone or PBS buffer. Pre-inoculation sera, as well as 3 and 6 week post-inoculation sera, were diluted 1:1000 fold and tested for IgG-specific antibody responses to MBP. (Inset) ELISA data for 1:100 dilution of serum collected at week 3-time point. *, **, and *** indicate *p* values of 0.005, 0.018 and 0.071 compared to MBP alone, respectively. Two animals, one from the MBP group and the other from the PBS group, died from unknown causes prior to final blood collection.